Synthesis, Structure and Magnetic Properties of Mn_{12} Single Molecule Magnet Containing 4-(Methylthio)benzoate as Peripheral Ligands

Jin Mook Lim, Youngkyu Do, and Jinkwon Kim[†,*]

Department of Chemistry, School of Molecular Science BK-21 and Center for Molecular Design and Synthesis, KAIST, Daejeon 305-701, Korea

[†]*Department of Chemistry, Kongju National University, Kongju, Chungnam 314-701, Korea.* [*]*E-mail: jkim@kongju.ac.kr*

Received December 7, 2004

$[Mn_{12}O_{12}(O_2CPh\text{-}4\text{-}SMe)_{16}(H_2O)_4]\cdot 7CH_2Cl_2$ (**1**), a new single-molecule magnet complex has been successfully synthesized by substitution of acetate ligand of Mn12ac with 4-(methylthio)benzoic acid. Complex **1** crystallizes into triclinic $P\bar{1}$ with a = 18.321(3) Å, b = 19.011(3) Å, c = 27.230(4) Å, α = 86.973(3)°, β = 76.919(3)°, γ = 87.613(3)°, and Z = 2. In complex **1**, one Mn(III) ion has an abnormal Jahn-Teller elongation axis oriented at an oxide ion. Complex **1** has two out-of-phase ac susceptibility peaks in the 2-4 K and 4-7 K regions. Effective anisotropy energy barrier and pre-exponential factor are U_{eff} = 45.95 K, $1/\tau_0 = 8.6 \times 10^9$ s^{-1} for χ_M" peaks in the lower temperature region and U_{eff} = 59.45 K, $1/\tau_0 = 2.2 \times 10^8$ s^{-1} for χ_M" peaks in the higher temperature region. The parameters of S = 10, g = 1.87, D = −0.40 cm^{-1}, and E = 0.00034 cm^{-1} were obtained from the M/Nμ_B *vs.* H/T plot of complex **1**.

Key Words : Single-molecule magnets, Manganese, Magnetic relaxation, 4-(Methylthio)benzoate

Introduction

There has been growing research interest in the field of single-molecule magnets (SMMs) after the discovery of $[Mn_{12}O_{12}(O_2CMe)_{16}(H_2O)_4]\cdot 2CH_3COOH\cdot 4H_2O$ ($Mn_{12}Ac$) which functions as a SMM below its blocking temperature.[1,2] SMM, as a prototype of nano-scale magnets, displays an intramolecular magnetic hysteresis loop; each independent molecule possesses the ability to function as a magnetizable magnet, owing to intrinsic intramolecular properties rather than intermolecular interactions and long-range ordering. In addition to a hysteresis behavior due to slow magnetization relaxation, Mn_{12} complexes exhibit steps on hysteresis loops due to resonant quantum tunneling.[3] Therefore, SMMs are regarded as the ultimate high-density memory devices[4] and quantum-computing application devices[5,6] in the future.

On the other hand, recent research reports showed that molecular clusters possessing quantized magnetic properties may provide powerful new systems for single-molecule electronics.[7,8] For such applications, it is essential to prepare properly oriented molecular films of SMMs onto a substrate. The first attempt to grow well-organized multilayer films of Mn12 SMM has been reported by using Langmuir-Blodgett (LB) technique.[9] Close packed lamellar structures with the Mn12 clusters organized in well-defined monolayers were obtained by that method. The second approach has been made by casting nanocomposite film consisting of polycarbonate and Mn12 complexes onto a glass surface.[10] However, there are limitations in those techniques, *i.e.* lack of stability of LB films due to incompatible surface energy and aggregations of clusters in nanocomposite method. Therefore, we designed a new Mn12 complex with functional groups in peripheral ligands to afford a molecular monolayer on metal surface. In particular, it is well known that sulfur-containing organic molecules are easily ordered in metal surface such as gold due to strong affinity of S toward Au. Herein we report synthesis, structure and magnetic properties of new Mn12-derivative that all acetate are fully substituted with 4-(methylthio)benzoic acid.

Experimental Section

All preparations and manipulations were performed under aerobic conditions; all chemicals and solvents were used as received. $[Mn_{12}O_{12}(O_2CMe)_{16}(H_2O)_4]\cdot 2CH_3COOH\cdot 4H_2O$ was prepared as reported.[11]

$[Mn_{12}O_{12}(O_2CPh\text{-}4\text{-}SMe)_{16}(H_2O)_4]\cdot 7CH_2Cl_2$ (1). To a slurry of $[Mn_{12}O_{12}(O_2CMe)_{16}(H_2O)_4]\cdot 2CH_3COOH\cdot 4H_2O$ (206 mg, 0.1 mmol) in CH_2Cl_2 (20 mL) was added 4-(methylthio)benzoic acid (270 mg, 1.6 mmol) and stirred for 4h at room temperature to give dark blown solution. After filtration, the solution was concentrated to remove acetic acid under vacuum. The resulting solid was dissolved in toluene and concentrated to remove residual acetic acid as the toluene azeotrope. This process repeated several times. The resulting dark brown powder was dissolved in CH_2Cl_2 and layered with pentane. Slow diffusion of the layers yielded dark brown crystals of **1**. Selected IR data (KBr, cm^{-1}): 3434 (w, b), 2919 (w), 1593 (s), 1536 (m), 1492 (m), 1408 (s), 1186 (m), 1090 (m), 769 (m), 692 (m), 658 (m), 618 (m), 551 (m).

X-ray Structure Determinations. A single crystal was coated with Paratone-N oil, attached to glass fibers, transferred to on a Bruker AXS SMART diffractometer equipped with a CCD detector in a nitrogen cold stream maintained at 150 K. More than a hemisphere of data was collected on each crystal over three batches of exposure using MoKα

Table 1. Details of the Crystallographic Data Collection for **1**

Chemical formula	$C_{135}H_{134}Cl_{14}Mn_{12}O_{48}S_{16}$
Chemical formula weight	4192.96
Temperature	150 K
Space group	$P\bar{1}$
Cryst size, mm	0.40 × 0.35 × 0.20
a, Å	18.321(3)
b, Å	19.011(3)
c, Å	27.230(4)
a, °	86.973(3)
b, °	76.919(3)
g, °	87.613(3)
V, Å^3	9221(2)
Z	2
ρ_{calcd}, g cm^{-3}	1.510
μ, mm^{-1}	1.246
λ (Mo Kα), Å	0.71073
θ range for data collection	1.35 to 28.14°
Index ranges	$-23\le h\le 23$, $-25\le k\le 25$, $-35\le l\le 35$
Reflection collected	79605
Independent reflections	40866 [R(int) = 0.1179]
Refinement method	Full-matrix least-squares on F^2
Data / restraints / parameters	40866 / 0 / 1860
Goodness-of-fit on F^2	0.971
Final R indices [I > 2σ(I)]	R_1 = 0.1067, wR_2 = 0.2685
Largest diff. peak and hole	2.304 and −1.866 e A^{-3}

radiation (λ = 0.71073 Å). A fourth set of data was measured and compared to the initial set to monitor and correct for decay, which was negligible in all cases. Data processing was then performed using the program SAINT.[12] The structure of the compound was solved by the direct method and refined by the full-matrix least-squares method on all F^2 data using SHELX 97.[13] The anisotropic thermal parameters for all non-hydrogen atoms but some disordered solvent molecules were included in the refinements. The phenyl rings of ligands were refined with a regular hexagon model. All hydrogen atoms bonded to carbon atoms were included in calculated positions. The C-H bond distances were fixed and the U values were assigned based approximately on the U value of the attached atom. The crystal and refinement data are summarized in Table 1.

Physical Measurement. Direct current (dc) and alternating current (ac) magnetic susceptibility measurements were carried out on a Quantum Design MPMS-*XL* magnetometer equipped with a 5 T magnet and operating in the range of 1.8-300 K. The ac susceptibility data were measured in the frequency range of 20-1500 Hz in the ac field strength of 3.0 G. Pascal's constants[14] were used to estimate the diamagnetic corrections for the complex. Infrared (IR) spectra were obtained in 4000 to 400 cm^{-1} range by Perkin-Elmer Spectrum 1000 spectrometer. The sample was ground with dry KBr and pressed into a transparent disk.

Results and Discussion

Synthesis. The ligand substitution reaction of $Mn_{12}Ac$ with 4-(methylthio)benzoic acid has been done by a modified azeotropic distillation method.[15] $Mn_{12}Ac$ was treated with stoichiometric amount of 4-(methylthio)benzoic acid in dichloromethane. The solubility of $Mn_{12}Ac$ is very poor in dichloromethane but as reacted with 4-(methylthio)benzoic acid the solution color changed to dark, indicating a formation of complex **1** which is good soluble in dichloromethane. To complete ligand substitution, toluene was added to the reaction mixture and evaporated to remove acetic acid as the toluene azeotrope, and the process repeated. Previously, most ligand substitution reactions have been done under the condition of large excess amount of RCOOH. However, by adapting of azeotropic distillation method, only stoichiometric amount of 4-(methylthio)benzoic acid is enough for complete ligand exchage reaction.

X-ray Structure: Complex **1** crystallizes in the space group P-1. An ORTEP diagram of $[Mn_{12}O_{12}(O_2CPh\text{-}4\text{-}SMe)_{16}(H_2O)_4]$ is shown in Figure 1. Selected bond distances and angles are listed in Table 2 and 3, respectively. The overall structural features of complex **1** are quite similar to the other $[Mn_{12}O_{12}]$ complexes:[11,15] The inner core $[Mn^{IV}{}_4O_4]^{8+}$ cubane unit is held within a non-planar ring of eight Mn^{III} atoms by eight μ_3-O^{2-} ions. The total of sixteen 4-(methylthio)benzoates bridge the outer-ring Mn atoms to the both the inner core and the other outer-ring Mn atoms. The four water molecules are located on the two Mn atoms to complete octahedral coordination; one H_2O each on the Mn(6) and Mn(8) atoms and two H_2O on the Mn(12) atom.

The Mn^{III}-O bonds of $[Mn_{12}O_{12}]$ complexes are tetragonally elongated due to a Jahn-Teller distortion. An elongation axis is usually parallel to the molecular C_2 axis in order to avoid the strong Mn(III)-O(oxo) bonds.[11,15] However, two equatorial bonds of Mn10-O11 [2.130(6) Å] and Mn10-O22

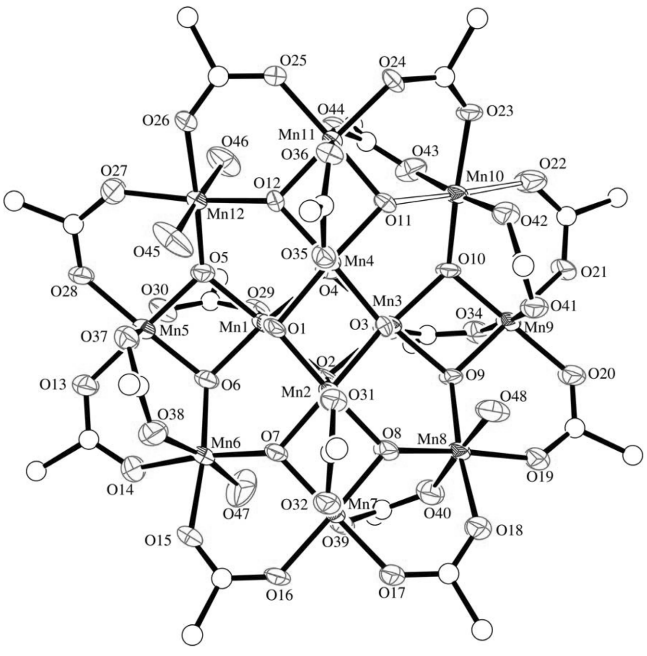

Figure 1. ORTEP diagram of complex **1**. 4-(methylthio)phenyl groups are omitted for clarity. Unusual Jahn-Teller elongation axis is emphasized with a different line drawing.

Table 2. Selected bond distances (Å) of **1**

A	B	distance	A	B	distance
Mn1	O1	1.933(6)	Mn1	O3	1.941(7)
Mn1	O4	1.883(6)	Mn1	O5	1.864(7)
Mn1	O6	1.870(6)	Mn1	O29	1.921(7)
Mn2	O2	1.922(6)	Mn2	O3	1.885(6)
Mn2	O4	1.887(6)	Mn2	O7	1.872(6)
Mn2	O8	1.879(7)	Mn2	O31	1.916(7)
Mn3	O1	1.907(7)	Mn3	O2	1.903(6)
Mn3	O3	1.911(6)	Mn3	O9	1.868(7)
Mn3	O10	1.869(6)	Mn3	O33	1.915(7)
Mn4	O1	1.901(6)	Mn4	O2	1.918(6)
Mn4	O4	1.976(6)	Mn4	O11	1.823(6)
Mn4	O12	1.868(6)	Mn4	O35	1.932(6)
Mn5	O5	1.908(6)	Mn5	O6	1.880(7)
Mn5	O13	1.950(7)	Mn5	O30	2.230(7)
Mn5	O28	1.920(7)	Mn5	O37	2.198(7)
Mn6	O6	1.887(6)	Mn6	O7	1.881(7)
Mn6	O14	1.935(8)	Mn6	O15	1.965(8)
Mn6	O38	2.109(8)	Mn6	O47	2.174(9)
Mn7	O7	1.907(7)	Mn7	O8	1.878(6)
Mn7	O16	1.915(7)	Mn7	O17	1.935(7)
Mn7	O32	2.219(7)	Mn7	O39	2.193(7)
Mn8	O8	1.870(6)	Mn8	O9	1.900(6)
Mn8	O18	1.974(7)	Mn8	O19	1.922(7)
Mn8	O40	2.089(8)	Mn8	O48	2.280(8)
Mn9	O9	1.908(6)	Mn9	O10	1.866(7)
Mn9	O20	1.950(8)	Mn9	O21	1.912(6)
Mn9	O34	2.223(8)	Mn9	O41	2.231(8)
Mn10	O10	1.882(6)	Mn10	O11	2.130(6)
Mn10	O22	2.176(7)	Mn10	O23	1.961(7)
Mn10	O42	1.936(8)	Mn10	O43	1.952(8)
Mn11	O11	1.858(7)	Mn11	O12	1.893(6)
Mn11	O24	1.936(6)	Mn11	O25	1.950(7)
Mn11	O36	2.194(7)	Mn11	O44	2.218(7)
Mn12	O5	1.889(7)	Mn12	O12	1.864(6)
Mn12	O26	1.929(7)	Mn12	O27	1.961(8)
Mn12	O45	2.202(8)	Mn12	O46	2.205(7)

[2.176(7) Å] are longer than the other equatorial and axial bonds as shown in Figure 1, *i.e.* one Jahn-Teller axis is abnormally perpendicular to molecular C_2 axis. This phenomenon of Jahn-Teller isomerism has been recently defined for $[Mn_{12}O_{12}(O_2CCH_2Bu^t)_{16}(H_2O)_4]$ and $[Mn_{12}O_{12}(O_2CC_6H_4\text{-}4\text{-}Me)_{16}(H_2O)_4]\cdot HO_2CC_6H_4\text{-}4\text{-}Me$.[16,17] The axial Mn-O(carboxylate) bonds [1.936(8) and 1.952(8) Å] and one equatorial Mn-O(carboxylate) bond [1.961(7) Å] at Mn(10) are normal lengths. The equatorial Mn-O(oxo) bond [1.882(6) Å] is quite shorter than the elongated Mn-O(oxo) bond [2.130(6) Å].

Magnetic Properties: Out-of-phase ac magnetic susceptibility (χ_M") measurements were carried out in the region of 2 to 10 K at different frequencies in 3.0 Oe ac field. As shown in Figure 2, complex **1** shows two frequency-dependent χ_M" peaks in the regions of 2-4 K and 4-7 K. Most Mn_{12} complexes have predominantly χ_M" peak in the 4-7 K

Table 3. Selected bond angles (°) of **1**

A	B	C	angle	A	B	C	angle
O5	Mn1	O6	84.1(3)	O5	Mn1	O4	87.9(3)
O6	Mn1	O4	92.5(3)	O5	Mn1	O29	91.0(3)
O6	Mn1	O29	93.5(3)	O4	Mn1	O29	173.8(3)
O5	Mn1	O1	101.7(3)	O6	Mn1	O1	173.6(3)
O4	Mn1	O1	85.1(3)	O29	Mn1	O1	89.1(3)
O5	Mn1	O3	170.7(3)	O6	Mn1	O3	95.0(3)
O4	Mn1	O3	82.8(3)	O29	Mn1	O3	98.3(3)
O1	Mn1	O3	78.9(3)	O7	Mn2	O8	83.7(3)
O7	Mn2	O3	88.8(3)	O8	Mn2	O3	92.2(3)
O7	Mn2	O4	98.5(3)	O8	Mn2	O4	175.7(3)
O3	Mn2	O4	84.2(3)	O7	Mn2	O31	95.1(3)
O8	Mn2	O31	89.9(3)	O3	Mn2	O31	175.8(3)
O4	Mn2	O31	93.5(3)	O7	Mn2	O2	172.5(3)
O8	Mn2	O2	96.2(3)	O3	Mn2	O2	83.8(3)
O4	Mn2	O2	81.1(3)	O31	Mn2	O2	92.3(3)
O9	Mn3	O10	83.6(3)	O9	Mn3	O2	89.0(3)
O10	Mn3	O2	95.8(3)	O9	Mn3	O1	171.7(3)
O10	Mn3	O1	96.2(3)	O2	Mn3	O1	82.8(3)
O9	Mn3	O3	99.9(3)	O10	Mn3	O3	176.5(3)
O2	Mn3	O3	83.6(3)	O1	Mn3	O3	80.3(3)
O9	Mn3	O33	93.2(3)	O10	Mn3	O33	92.2(3)
O2	Mn3	O33	171.9(3)	O1	Mn3	O33	95.1(3)
O3	Mn3	O33	88.3(3)	O11	Mn4	O12	85.0(3)
O11	Mn4	O1	91.6(3)	O12	Mn4	O1	89.3(3)
O11	Mn4	O2	97.3(3)	O12	Mn4	O2	171.6(3)
O1	Mn4	O2	82.6(3)	O11	Mn4	O35	95.4(3)
O12	Mn4	O35	90.5(3)	O1	Mn4	O35	172.9(3)
O2	Mn4	O35	97.4(3)	O11	Mn4	O4	174.2(3)
O12	Mn4	O4	98.1(3)	O1	Mn4	O4	83.5(2)
O2	Mn4	O4	79.0(3)	O35	Mn4	O4	89.6(3)
O6	Mn5	O5	82.6(3)	O6	Mn5	O28	177.1(3)
O5	Mn5	O28	95.7(3)	O6	Mn5	O13	96.7(3)
O5	Mn5	O13	176.9(3)	O28	Mn5	O13	84.8(3)
O6	Mn5	O37	94.4(3)	O5	Mn5	O37	91.4(3)
O28	Mn5	O37	88.0(3)	O13	Mn5	O37	91.6(3)
O6	Mn5	O30	88.1(3)	O5	Mn5	O30	82.7(3)
O28	Mn5	O30	89.4(3)	O13	Mn5	O30	94.2(3)
O37	Mn5	O30	173.3(3)	O7	Mn6	O6	94.9(3)
O7	Mn6	O14	172.9(3)	O6	Mn6	O14	91.1(3)
O7	Mn6	O15	91.0(3)	O6	Mn6	O15	173.4(3)
O14	Mn6	O15	83.2(4)	O7	Mn6	O38	93.9(3)
O6	Mn6	O38	93.0(3)	O14	Mn6	O38	89.7(4)
O15	Mn6	O38	83.6(4)	O7	Mn6	O47	93.2(3)
O6	Mn6	O47	92.8(3)	O14	Mn6	O47	82.6(4)
O15	Mn6	O47	89.7(4)	O38	Mn6	O47	170.4(4)
O8	Mn7	O7	82.9(3)	O8	Mn7	O16	175.8(3)
O7	Mn7	O16	95.3(3)	O8	Mn7	O17	96.2(3)
O7	Mn7	O17	173.6(3)	O16	Mn7	O17	85.2(3)
O8	Mn7	O39	92.3(3)	O7	Mn7	O39	97.2(3)
O16	Mn7	O39	91.7(3)	O17	Mn7	O39	89.2(3)
O8	Mn7	O32	86.7(3)	O7	Mn7	O32	83.7(3)
O16	Mn7	O32	89.3(3)	O17	Mn7	O32	89.9(3)
O39	Mn7	O32	178.5(3)	O8	Mn8	O9	94.4(3)
O8	Mn8	O19	171.1(3)	O9	Mn8	O19	92.9(3)

Table 3. Continued

A	B	C	angle	A	B	C	angle
O8	Mn8	O18	90.6(3)	O9	Mn8	O18	173.3(3)
O19	Mn8	O18	81.8(3)	O8	Mn8	O40	94.9(3)
O9	Mn8	O40	94.4(3)	O19	Mn8	O40	89.6(3)
O18	Mn8	O40	89.7(3)	O8	Mn8	O48	83.9(3)
O9	Mn8	O48	90.1(3)	O19	Mn8	O48	91.0(3)
O18	Mn8	O48	85.9(3)	O40	Mn8	O48	175.4(3)
O10	Mn9	O9	82.5(3)	O10	Mn9	O21	98.4(3)
O9	Mn9	O21	174.5(3)	O10	Mn9	O20	175.1(3)
O9	Mn9	O20	96.6(3)	O21	Mn9	O20	82.9(3)
O10	Mn9	O34	87.5(3)	O9	Mn9	O34	84.7(3)
O21	Mn9	O34	89.9(3)	O20	Mn9	O34	97.2(3)
O10	Mn9	O41	88.0(3)	O9	Mn9	O41	93.1(3)
O21	Mn9	O41	92.4(3)	O20	Mn9	O41	87.3(3)
O34	Mn9	O41	175.2(3)	O10	Mn10	O42	93.9(3)
O10	Mn10	O43	90.2(3)	O42	Mn10	O43	175.4(3)
O10	Mn10	O23	175.5(3)	O42	Mn10	O23	86.1(3)
O43	Mn10	O23	89.7(3)	O10	Mn10	O11	91.7(3)
O42	Mn10	O11	85.0(3)	O43	Mn10	O11	96.9(3)
O23	Mn10	O11	92.8(3)	O10	Mn10	O22	92.1(3)
O42	Mn10	O22	91.2(3)	O43	Mn10	O22	86.5(3)
O23	Mn10	O22	83.4(3)	O11	Mn10	O22	174.9(3)
O11	Mn11	O12	83.3(3)	O11	Mn11	O24	94.8(3)
O12	Mn11	O24	175.5(3)	O11	Mn11	O25	177.7(3)
O12	Mn11	O25	95.0(3)	O24	Mn11	O25	87.0(3)
O11	Mn11	O36	87.3(3)	O12	Mn11	O36	86.4(3)
O24	Mn11	O36	89.5(3)	O25	Mn11	O36	94.1(3)
O11	Mn11	O44	93.0(3)	O12	Mn11	O44	93.0(3)
O24	Mn11	O44	91.2(3)	O25	Mn11	O44	85.5(3)
O36	Mn11	O44	179.2(3)	O12	Mn12	O5	93.5(3)
O12	Mn12	O26	90.5(3)	O5	Mn12	O26	174.9(3)
O12	Mn12	O27	171.8(3)	O5	Mn12	O27	94.3(3)
O26	Mn12	O27	81.9(3)	O12	Mn12	O45	87.5(3)
O5	Mn12	O45	92.5(3)	O26	Mn12	O45	90.8(3)
O27	Mn12	O45	89.5(4)	O12	Mn12	O46	89.7(3)
O5	Mn12	O46	88.8(3)	O26	Mn12	O46	88.0(3)
O27	Mn12	O46	93.2(3)	O45	Mn12	O46	177.0(3)
Mn2	O3	Mn3	95.8(3)	Mn2	O3	Mn1	94.8(3)
Mn3	O3	Mn1	100.2(3)	Mn4	O1	Mn3	96.7(3)
Mn4	O1	Mn1	94.8(3)	Mn3	O1	Mn1	100.6(3)
Mn1	O4	Mn2	96.7(3)	Mn1	O4	Mn4	94.0(2)
Mn2	O4	Mn4	99.5(3)	Mn3	O2	Mn4	96.3(3)
Mn3	O2	Mn2	94.9(3)	Mn4	O2	Mn2	100.4(3)
Mn1	O5	Mn12	132.7(4)	Mn1	O5	Mn5	95.6(3)
Mn12	O5	Mn5	128.2(4)	Mn1	O6	Mn5	96.4(3)
Mn1	O6	Mn6	132.7(4)	Mn5	O6	Mn6	123.1(3)
Mn2	O7	Mn6	132.8(4)	Mn2	O7	Mn7	95.6(3)
Mn6	O7	Mn7	126.6(3)	Mn8	O8	Mn7	125.1(4)
Mn8	O8	Mn2	133.2(3)	Mn7	O8	Mn2	96.4(3)
Mn3	O9	Mn8	132.6(3)	Mn3	O9	Mn9	95.4(3)
Mn8	O9	Mn9	128.8(4)	Mn9	O10	Mn3	96.8(3)
Mn9	O10	Mn10	125.1(4)	Mn3	O10	Mn10	133.7(4)
Mn4	O11	Mn11	96.4(3)	Mn4	O11	Mn10	131.6(3)
Mn11	O11	Mn10	117.9(3)	Mn12	O12	Mn4	132.9(3)
Mn12	O12	Mn11	132.5(3)	Mn4	O12	Mn11	93.7(3)

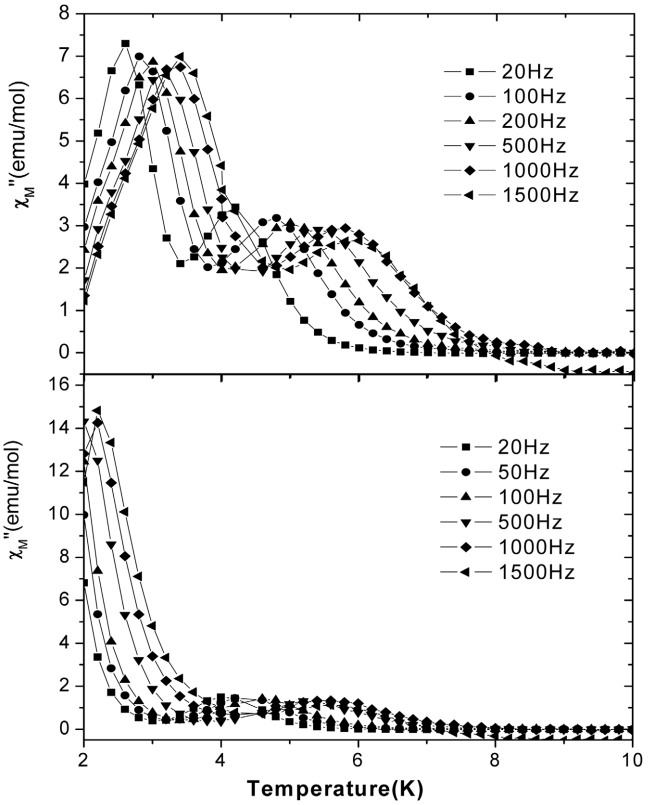

Figure 2. Comparison of out-of phase ac susceptibility signals of complex **1** (top) and completely dried sample of **1** (bottom).

region. Recent investigations have demonstrated that Jahn-Teller isomerism is a crucial source of a faster magnetization relaxation (*i.e.* χ_M" peak in the low temperature region).[16,17] A potential-energy barrier between spin-up and spin-down orientations of the magnetic moment of an individual Mn_{12} complex is decreased with decreasing of magnetic anisotropy due to a Jahn-Teller elongation perpendicular to C_2 axis. The complex $[Mn_{12}O_{12}(O_2CC_6H_4\text{-}4\text{-}Me)_{16}(H_2O)_4]\cdot HO_2CC_6H_4\text{-}4\text{-}Me$ has an equatorial Jahn-Teller elongated axis and predominantly a peak in the region of 2-4 K.[18] However, complex **1** has peaks in both lower and higher temperature regions with 2 : 1 intensity ratio. Almost the same χ_M" *vs* T plot was observed in the complex $[Mn_{12}O_{12}(O_2CC_6H_4\text{-}4\text{-}Cl)_{16}(H_2O)_4]\cdot 8CH_2Cl_2$ (**2**) which does not show Jahn-Teller isomerism.[17] Another example showing the same ac behavior is $[Mn_{12}O_{12}(O_2CCH_2CH_2Cl)_{16}(H_2O)_4]\cdot CH_2ClCH_2CO_2H$ (**3**) which also does not show any evidence of Jahn-Teller isomerism.[19] G. Christou *et al.* insisted that Jahn-Teller isomerism is believed to be the origin of the faster magnetization relaxation of some Mn_{12} complexes.[17] But the evidences observed in complexes **1**-**3** suggest that Jahn-Teller isomerism is not the only origin of the faster magnetization relaxation behaviors.

Magnetization relaxation rates ($1/\tau$) and effective anisotropy energy barriers were calculated from the theoretical equation given by

$$\ln(1/\tau) = -U_{eff}/kT + \ln(1/\tau_0) \quad (1)$$

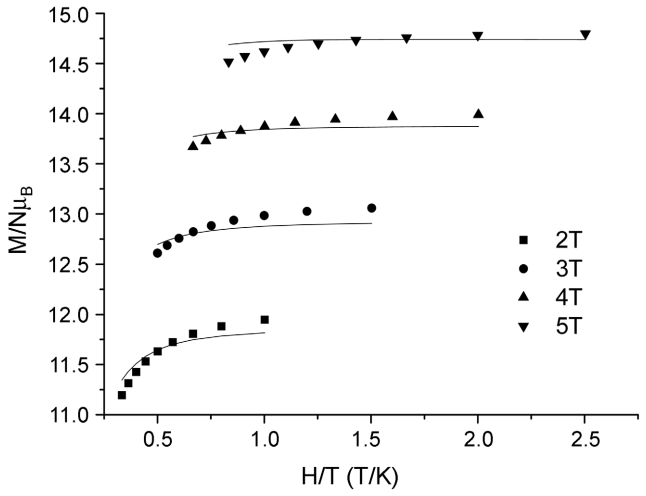

Figure 3. Plot of $M/N_{\mu B}$ *vs* H/T for complex **1** at the indicated applied fields. The solid lines are fits of the data.

where U_{eff} is the effective anisotropy energy barrier, k is the Boltzmann constant, and T is the temperature. Magnetic relaxation times (τ) are obtained from the relationship $\omega\tau = 1$ at the maxima of the χ_M" *vs*. T plots. Peak maxima are accurately determined by fitting the peaks to a Lorentzian function. A least-squares fit of ac susceptibility relaxation data to equation 1 gives $U_{eff\text{-}low} = 45.95$ K, $1/\tau_0 = 8.6 \times 10^9$ s^{-1} for the faster relaxation and $U_{eff\text{-}high} = 59.45$ K, $1/\tau_0 = 2.2 \times 10^8$ s^{-1} for the slower relaxation. The U_{eff} value for slower relaxation is slightly smaller than the normal range 60-70 K observed previously for several Mn_{12} complexes.[3]

Solvate molecules in crystal lattice of Mn_{12} complexes seem to play an important role in relaxation process. It is interesting to note that the χ_M" peak height in the higher temperature region is decreased whereas the peak height in the lower temperature range is increased as complex **1** loses solvate molecules. This behavior can be interpreted in a way that transverse anisotropy is increased because losing solvate molecules from crystal lattice causes increasing in structural disorder of Mn_{12} molecules in crystal lattice. The sample of complex **1** dried overnight under vacuum exhibits predominantly an out-of-phase susceptibility peak in the lower temperature region as shown in Figure 2 (bottom).

Reduce magnetization measurement (Figure 3) of dried sample of **1** was done in the range of 2-5 T in the 2.0-6.0 K region and data were fitted using the program ANISOFIT[20] to give $S = 10$, $g = 1.87$, $D = -0.40$ cm^{-1}, and $E = 0.00034$ cm^{-1}, where D is the axial zero field splitting (ZFC) parameter and E is the rhombic ZFC parameter. The D value is comparable with the value obtained from the equation **1** for the faster relaxation.

Hysteresis loops for complex **1** (left) and dried sample of **1** (right) at 2 K are shown in Figure 4 (top). The dried samples shows smaller coersive field. Small plateaus for both complexes are observed in hysteresis loops because of quantum tunneling of magnetization (QTM). To clarify the positions of QTM plots of dM/dH *vs*. H are drawn in Figure 4 (bottom). QTM is occurred at a field of each peak.

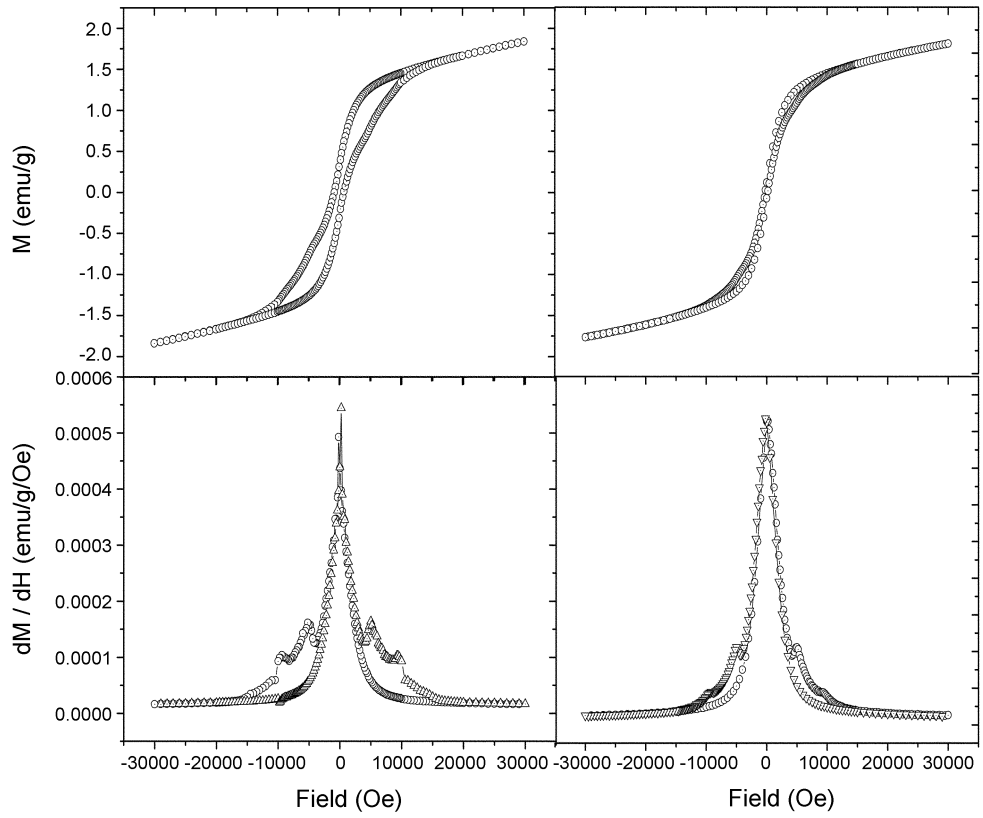

Figure 4. Comparison of hysteresis loops of complex **1** and dried sample of complex **1** at 2 K.

Conclusion

A new single molecule magnet Mn_{12} complex containing sulfur atom in its peripheral ligands was successfully synthesized by ligand substitution reaction. Complex **1** shows Jahn-Teller isomerism in molecular structure and two out-of-phase ac susceptibility peaks in both 2-4 K and 4-7 K regions. The dried sample of **1** has predominantly peaks in lower temperature range. These facts indicate that the faster magnetization relaxation is not caused only by Jahn-Teller isomerism but by several conditions such as structure disorder due to losing solvate molecules including Jahn-Teller isomerism.

Acknowledement. This work was supported by the ministry of science and technology, Korea (NRL program).

Supplementary Materials. Crystallographic data for **1** are available from the corresponding author upon request and via the internet at *http://www.kcsnet.or.kr/bkcs*.

References

1. Sessoli, R.; Gatteschi, D.; Caneschi, A.; Novak, M. A. *Nature* **1993**, *365*, 141.
2. Sessoli, R.; Tsai, H.-L.; Schake, A. R.; Wang, S.; Vincent, J. B.; Folting, K.; Gatteschi, D.; Christou, G.; Hendrickson, D. N. *J. Am. Chem. Soc*. **1993**, *115*, 1804.
3. (a) Thomas, L.; Lionti, F.; Ballou, R.; Gatteschi, D.; Sessoli, R.; Babara, B. *Nature* **1996**, *383*, 145. (b) Friedman, J. R.; Sarachik, M. P.; Tejada, J.; Ziolo, R. *Phys. Rev. Lett.* **1996**, *76*, 3830. (c) Sangregorio, C.; Ohm, T.; Paulsen, C.; Sessoli, R.; Gatteschi, D. *Phys. Rev. Lett.* **1997**, *78*, 4645. (d) Aubin, S. M. J.; Dilley, N. R.; Wemple, M. B.; Christou, G.; Hendrickson, D. N. *J. Am. Chem. Soc.* **1998**, *120*, 839. (e) Aubin, S. M. J.; Dilley, N. R.; Wemple, M. B.; Christou, G.; Hendrickson, D. N. *J. Am. Chem. Soc.* **1998**, *120*, 4991. (f) Wernsdorfer, W.; Sessoli, R. *Science* **1999**, *284*, 133. (g) Gatteschi, D.; Sessoli, R. *Angew. Chem. Int. Ed.* **2003**, *42*, 268.
4. (a) Dahlberg, E. D.; Zhu, J. G. *Phys. Today* **1995**, 34. (b) McMichael, R. D.; Shull, R. D.; Swatzendruber, L. J.; Bennett, J. H.; Watson, R. E. *J. Magn. Magn. Mater.* **1992**, *111*, 29. (c) Awschalom, D. D.; DiVincenzo, D. P.; Smith, F. F. *Science* **1992**, *258*, 414. (d) Christou, G.; Gatteschi, D.; Hendrickson, D. N.; Sessoli, R. *MRS Bull.* **2000**, *25*, 66.
5. (a) Leuenberger, M. N.; Loss, D. *Nature* **2001**, *410*, 789. (b) Zhou, B.; Tao, R.; Shen, S.-Q.; Liang, J.-Q. *Phys. Rev. A* **2002**, *66*, 010301.
6. (a) Makhlin, Y.; Schon, G.; Shnirman, A. *Nature* **1999**, *398*, 305. (b) Tejada, J.; Chudnovsky, E. M.; del Barco, E.; Hernandez, J. M.; Spiller, T. P. *Nanotechnology* **2001**, *12*, 181.
7. Kim, G.-H.; Kim, T.-S. *Phys. Rev. Lett.* **2004**, *92*, 137203.
8. Liang, W.; Shores, M. P.; Bockrath, M.; Long, J. R.; Park, H. *Nature* **2002**, *417*, 725
9. Clemente-León, M.; Soyer, H.; Coronado, E.; Mingotaud, C.; Gómez-García, C. J.; Delhaès, P. *Angew. Chem. Int. Ed.* **1998**, *37*, 2841.
10. Ruiz-Molina, D.; Mas-Torrent, M.; Gomez, J.; Balana, A. I.; Domingo, N.; Tejada, J.; Martinez, M. T.; Rovira, C.; Veciana, J. *Adv. Mater.* **2003**, *15*, 42.
11. Lis, T. *Acta Crystallogr.* **1980**, *B36*, 2042.
12. SAI*NT-Plus*, version 6.02; Bruker Analytical X-ray System: Madison, WI, 1999.
13. Sheldrick, G. M. *SHELX 97*; Universität of Göttingen: Göttingen, Germany, 1997.
14. *Theory and Application of Molecular Paramagnetism*; Boudreaux, E. A., Mulay, L. N., Eds.; Wiley and Sons: New York, 1976.
15. (a) Eppley, H. J.; Tsai, H.-L.; de Vries, N.; Folting, K.; Christou, G.; Hendrickson, D. N. *J. Am. Chem. Soc.* **1995**, *117*, 301. (b) Jeon, W.; Jin, M. K.; Kim, Y.; Jung, D.-Y.; Suh, B. J.; Yoon, S. *Bull. Korean Chem. Soc.* **2004**, *25*, 1036.
16. Sun, Z.; Ruiz, D.; Dilley, N. R.; Soler, M.; Ribas, J.; Guzei, I. A.; Rheingold, A. L.; Folting, K.; Maple, M. B.; Christou, G.; Hendrickson, D. N. *Chem. Commun.* **1999**, 1973.
17. Aubin, S. M. J.; Sun, Z.; Eppley, H. J.; Rumberger, E. M.; Guzei, I. A.; Folting, K.; Gantzel, P. K.; Rheingold, A. L.; Christou, G.; Hendrickson, D. N. *Inorg. Chem*. **2001**, *40*, 2127.
18. Aubin, S. M. J.; Sun, Z.; Guzei, I. A.; Rheingold, A. L.; Christou, G.; Hendrickson, D. N. *Chem. Commun.* **1997**, 2239.
19. Park, C.-D.; Rhee, S. W.; Kim, Y.; Jeon, W.; Jung, D.-Y.; Kim, D.; Do, Y.; Ri, H.-C. *Bull. Korean Chem. Soc.* **2001**, *22*, 453.
20. Shores, M. P.; Sokol, J. J.; Long, J. R. *J. Am. Chem. Soc.* **2002**, *124*, 2279.